Metal-Dielectric Thin Film Structure Metamaterial for Obtaining High Equilibrium Temperature Under Direct Solar Optical Radiation

Jinnan Chen and Junpeng Guo, *Senior Member, IEEE*

***Abstract*—Metal-dielectric thin film structure metamaterials can be designed to absorb solar light radiation over a wide spectral band. By using Kirchhoff's law, metal-dielectric thin film metamaterials are investigated for obtaining high equilibrium temperatures under direct solar light radiation at normal incidence. It is found that among all metal-dielectric thin film structures, the dielectric layer on metal (DLM) surface structure is the optimal structure for producing the highest thermal equilibrium temperature under direct solar optical radiation.**

***Index Terms*—Thin film coatings, metamaterial, optical properties of photonic materials.**

I. Introduction

SOLAR Light absorbers are critical elements for solar thermal energy harvesting systems. Ideally, solar light absorbers are preferred to have unit absorptance over the wideband solar light spectrum, and zero thermal emission in the long-wavelength infrared spectral tail [1]–[3]. Metal-dielectric multilayer thin film structures have been extensively investigated for wideband solar light absorption because of the low cost lithography-free fabrication [4]–[14]. Practically, it is easy to obtain wideband solar light absorption in visible spectrum, but difficult to completely suppress thermal emission in the infrared region. Previously, various multilayer thin film structures have been reported for obtaining wideband solar light absorption [4]–[14] and thermal emission control [15]–[20]. For solar energy systems, the temperature of a solar light absorber affects the efficiency of the system [15], [21]–[23]. However, equilibrium temperature of multilayer thin film structure metamaterials under direct solar light radiation has not yet been investigated

In this work, equilibrium temperatures of metal-dielectric thin film structures are calculated by using Kirchhoff's law and law of energy conservation. The motivation of this research is to find the optimal thin film structure that can produce the highest equilibrium temperature under direct solar optical radiation without concentration. The method in this paper can also be applied to predict equilibrium temperatures of other material systems for solar energy harvesting and radiative cooling applications.

Manuscript received January 3, 2022; revised January 28, 2022; accepted January 28, 2022. Date of publication February 4, 2022; date of current version February 15, 2022. This work was supported by Alabama Graduate Research Scholarship Program under Grant ACHE-GRSP-UAH-10/11. *(Corresponding author: Junpeng Guo.)*

The authors are with the Department of Electrical and Computer Engineering, The University of Alabama in Huntsville, Huntsville, AL 35899 USA (e-mail: jc0082@uah.edu; guoj@uah.edu).

Digital Object Identifier 10.1109/JPHOT.2022.3148255

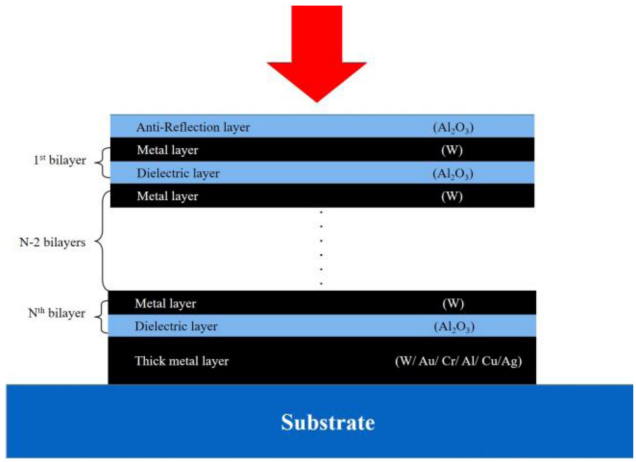

Fig. 1. Metal-dielectric thin film metamaterial structure. A metal-dielectric bilayer as a unit cell, repeats N times to form a multilayer thin film structure on an opaque thick metal film on a substrate. A dielectric layer on the top of the metal-dielectric bilayer structure functions as an anti-reflection layer. When N = 0, only a single dielectric layer is on the bottom thick metal layer surface.

II. Metal-Dielectric Thin Film Metamaterial and Calculation of Directional Thermal Emissivity

The metal-dielectric thin film structure investigated in this work is illustrated in Fig. 1. At the top, a thin film of aluminum oxide (Al_2O_3) dielectric is used as an anti-reflection (AR) layer to reduce the optical reflection and simultaneously protect the surface. Tungsten (W) is used as the metal film material, and aluminum oxide (Al_2O_3) is used as the dielectric layer material. A tungsten layer and an aluminum oxide layer form a metal-dielectric bilayer, stacking together to form a multilayer thin film structure to enhance light absorption over the solar optical spectrum. The number of metal-dielectric bilayers *N*, is indicated in the diagram. Underneath the metal-dielectric bilayers is an optically thick metal layer which prevents light transmission to the substrate. Underneath the thick metal layer is the substrate. The choice of substrate material does not affect optical property of the structure since there is no light getting into the substrate. When $N = 0$, only a single dielectric layer is on the thick metal film surface. We call this structure as dielectric layer on metal (DLM) light absorbing structure.

To find the equilibrium temperature under direct solar optical radiation, we need to know the thermal emissivity of the thin

film structure surface in all radiation directions. According to Kirchhoff's thermal radiation law, emissivity of a surface in a given direction equals the optical absorptance in same direction [24]–[27]. Therefore, we need to calculate optical absorptance *A(θ, λ)* in all radiation directions at all wavelengths. Optical absorptance *A(θ, λ)* of the metal-dielectric multilayer thin-film structure can be calculated by using the transfer matrix method [28]. The transfer matrix is obtained from dynamical matrixes and the propagation matrixes of each layer of the structure. For TE polarization light, the dynamical matrix D_{si} of the medium *i* is,

$$D_{si} = \begin{bmatrix} 1 & 1 \\ n_i \cos\theta_i & -n_i \cos\theta_i \end{bmatrix}, \tag{1}$$

where θ_i is the angle of incidence in the medium *i,* n_i is the refractive index of the *i-th* medium, and *i = 1, 2, 3, …N.* For TM polarization light, the dynamical matrix D_{pi} of medium *i* is,

$$D_{pi} = \begin{bmatrix} n_i \cos\theta_i & n_i \cos\theta_i \\ 1 & -1 \end{bmatrix}, \tag{2}$$

where θ_i is the angle of incidence in the medium *i,* n_i is the refractive index of medium *i,* and *i = 1, 2, 3, …N.*

The propagation matrix regardless of polarizations in the medium *i* is,

$$P_i = \begin{bmatrix} e^{j\frac{2\pi n_i d_i}{\lambda}} & 0 \\ 0 & e^{-j\frac{2\pi n_i d_i}{\lambda}} \end{bmatrix}, \tag{3}$$

where n_i is the refractive index and d_i is the layer thickness of the medium *i*, λ is the free space wavelength, *j* is the imaginary number, and *i = 1, 2, 3, …N.*

The transfer matrix of the metal-dielectric thin film structure is,

$$M = D_0^{-1} D_{AR} P_{AR} D_{AR}^{-1} \left[D_m P_m D_m^{-1} D_d P_d D_d^{-1} \right]^N D_s, \tag{4}$$

$$M = \begin{bmatrix} M_{11} & M_{12} \\ M_{21} & M_{22} \end{bmatrix}, \tag{5}$$

In above equations, $D_{0,}$ is the dynamical matrix of the incident medium (air), D_{AR} is the dynamical matrix of the anti-reflection layer, D_m is the dynamical matrix of the metal layer, D_d is the dynamical matrix of the dielectric layer, and D_s is the dynamical matrix of the optically thick metal layer. P_{AR}, P_m, and P_d are propagation matrices of the anti-reflection layer, metal layer, and dielectric layer, respectively. The optical reflectance *R* from the thin film structure can be obtained from the elements of the transfer matrix of M in (5),

$$R = \left| \frac{M_{21}}{M_{11}} \right|^2, \tag{6}$$

The transmittance through this thin film structure is zero because the optically thick metal layer prohibits light transmission. Therefore, optical absorptance (A) can be calculated by using the law of energy conservation, i. e., *A = 1 - R*. Since the solar optical radiations are unpolarized light, the optical absorptance at wavelength λ and angle of incidence *θ,* is the average of the absorptance of TE polarization light $A_{TE}(\theta, \lambda)$ and absorptance of TM polarization light $A_{TM}(\theta, \lambda)$,

$$A\ (\theta, \lambda) = \frac{1}{2}\ \left[A_{TE}\,(\theta, \lambda) + A_{TM}\,(\theta, \lambda) \right], \tag{7}$$

A(θ, λ) is the angular and wavelength dependent optical absorptance for unpolarized solar optical radiation in the thin film structure metamaterial.

III. Thermal Emissivity of Metal-Dielectric Thin Film Structure Metamaterials

With transfer matrix method described in previous section, we first calculate the optical absorptance of the thin film structures with different number of bilayers *N = 0, 1, 2, 4, 6,* and *8* at different wavelengths and different angles of incidence for TE and TM polarization lights. The optical absorptance of unpolarized light is the average of the optical absorptance for TE and TM polarization lights. In our calculations, the tungsten metal layer thickness is chosen at 5 nm and the aluminum oxide dielectric layer thickness is chosen at 50 nm in the bilayer unit cell. The tungsten layer thickness in bottom is chosen as 200 nm, which is thick enough to block light transmission to the substrate in the spectral range of interest. Optical constants of tungsten metal and aluminum oxide dielectric film used in the calculation are taken from reference [29]. From calculated optical absorptance results, surface thermal emissivity can be obtained by applying the Kirchhoff's thermal radiation law.

Kirchhoff's thermal radiation law states that the thermal emissivity of a surface in a specific direction equals the absorptance in that direction [24]–[27]. Therefore, surface thermal emissivity $\varepsilon(\theta, \lambda)$ can be obtained from the calculated optical absorptance for unpolarized light, i. e.,

$$\varepsilon\ (\theta, \lambda) = \ \mathrm{A}\,(\theta, \lambda)\,, \tag{8}$$

Since the Kirchhoff's law states that thermal emissivity equals the optical absorptance, we first calculated the optical absorptance versus wavelength λ and angle of incidence *θ* for both TE and TM polarizations of light respectively. The optical absorptance of unpolarized solar light is the average of the optical absorptance of TE and TM polarization lights. The results are shown in Fig. 2 for structures with different number of bilayers *N = 0, 1, 2, 4, 6,* and *8*. It can be seen that the single dielectric layer on metal (DLM) structure surface can give over 80% emissivity over a wavelength range from 0.3 μm to 0.6 μm for incident angles below 75 degrees, while a four bilayer structure gives over 90% thermal emissivity in the wavelength range from 0.25 μm to 1.85 μm. The total thermal emissivity increases as the number of bilayers increases. It also can be seen in Fig. 2 that the single dielectric film on the metal structure gives almost zero thermal emissivity at the wavelength of 10 μm at large angles of incidence, while a six bilayer structure gives 0.40 thermal emissivity in the same spectral range. The results in Fig. 2 show that the thin film structures with large numbers of metal-dielectric bilayers have larger thermal emissivity over a wider spectral band than bilayer structures of small number of bilayers.

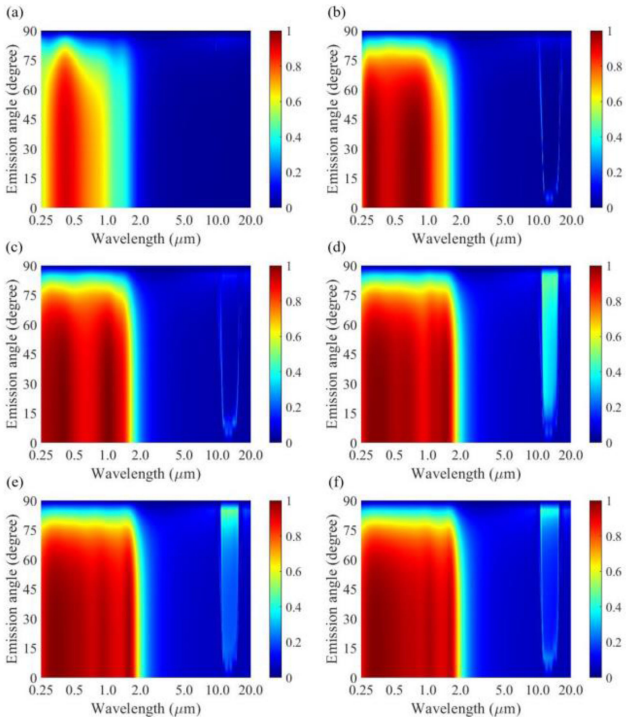

Fig. 2. Calculated thermal emissivity versus wavelength and emission angle for structures with different number of metal-dielectric bilayers: (a) N = 0, (b) N = 1, (c) N = 2, (d) N = 4, (e) N = 6, and (f) N = 8, respectively. For N = 0, only a single aluminum oxide dielectric film is on the tungsten metal surface.

IV. Equilibrium Temperatures of Thin Film Structure Metamaterials

With calculated angular dependent thermal emissivity data in previous section, total thermal emission power P_r from the surface can be obtained by integrating over all emission angles of a semi-sphere,

$$P_r = \int_0^{2\pi} d\varphi \int_0^{\frac{\pi}{2}} sin\theta d\theta \int_0^{\infty} \varepsilon(\theta,\lambda)\ L_{bb}(\lambda,T)\, d\lambda, \quad (9)$$

where θ is the observation polar angle and φ is the azimuthal angle. In the above equation, $L_{bb}(\lambda,T)$ is Planck's black body radiation spectrum at equilibrium temperature T,

$$L_{bb}\ (\lambda,T) = \frac{2hc^2}{\lambda^5}\ \frac{1}{exp\left(\frac{hc}{\lambda k_B T}\right)-1}, \quad (10)$$

where h is Planck's constant, c is the speed of light, k_B is the Boltzmann constant [30].

The absorbed solar radiation power can be calculated by using the optical absorptance of the surface and the measured solar irradiance on earth [31]. Assuming that the solar light radiation is at the normal direction, the absorbed solar radiation power is,

$$P_s = \int_0^{\infty} A_0(\lambda)\ L_{sun}(\lambda)\, d\lambda, \quad (11)$$

where λ is the optical wavelength, $A_0(\lambda)$ is the optical absorptance at normal incidence, and $L_{sun}(\lambda)$ is solar irradiance on surface of the earth [31].

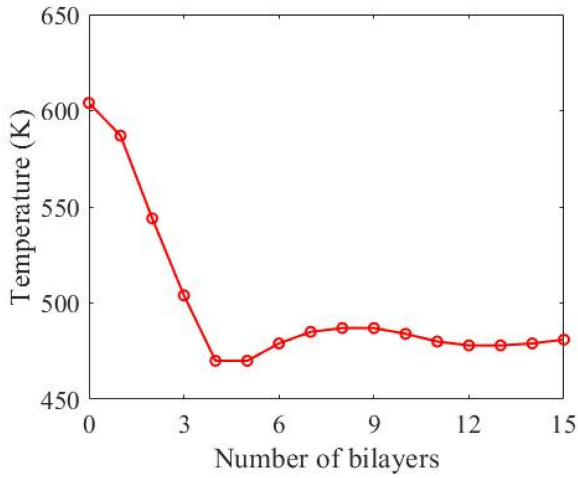

Fig. 3. Equilibrium temperature of metal-dielectric multilayer thin film metamaterial versus the number of metal-dielectric bilayers. The equilibrium temperature decreases as the number of metal-dielectric bilayers increases.

Assuming that the bottom of the thin film metamaterial is completely insulated from its surroundings, the total absorbed solar power is equal to the total thermal emission power at the equilibrium temperature because of energy conservation. By using the law of energy conservation, the equilibrium temperatures of the solar light absorber can be calculated. First, equilibrium temperatures of metal-dielectric thin film structures are calculated for different number of metal-dielectric bilayers. The equilibrium temperature of the multilayer thin film absorber is calculated for different numbers of bilayers, as shown in Fig. 3. The result indicates that the highest equilibrium temperature is 604 K for a zero-bilayer structure. A three-bilayer structure can have an equilibrium temperature of 504 K, while a six-bilayer structure can have an equilibrium temperature of 479 K. Increasing the number of bilayers results in a higher optical absorption in the short wavelength region, but also increases thermal emission in the infrared region and causes a large amount of energy loss. Therefore, equilibrium temperature cannot be increased by increasing the number of bilayers. A zero-bilayer structure can produce the highest equilibrium temperature under direct solar light radiation.

V. Equilibrium Temperature of Single Dielectric Film on Metal Surface Structure

It has been known previously that low thermal emissivity in the long wavelength spectral region is more critical than high absorptance in the short wavelength region for a solar light absorber to reach high equilibrium temperature [2], [3]. From Fig. 2, it is seen that the single dielectric layer on the metal surface has low thermal radiation than the multilayer structure in long wavelength region as well as the narrow absorption band and the low optical absorptance in the short wavelength region. Therefore, the single anti-reflection layer on the metal surface might be the best structure for achieving the highest equilibrium temperature. For this reason, we calculate the thermal emissivity of the zero-bilayer structure with different anti-reflection

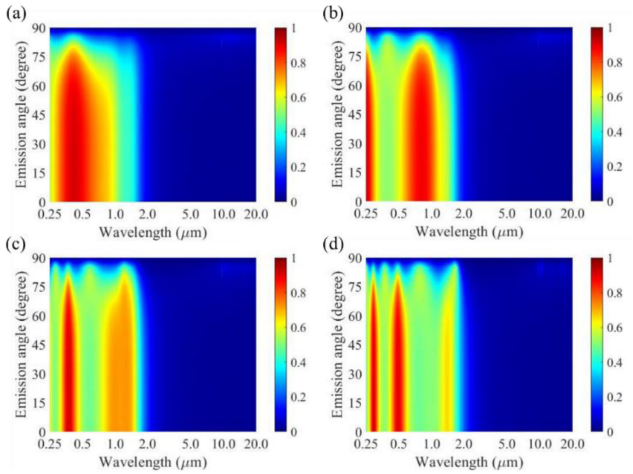

Fig. 4. Thermal emissivity versus wavelength and angle of emission for the dielectric layer on metal structure with different aluminum oxide dielectric layer thickness of (a) 50 nm, (b) 70 nm, (c) 90 nm, and (d) 110 nm. The bottom thick layer metal is tungsten.

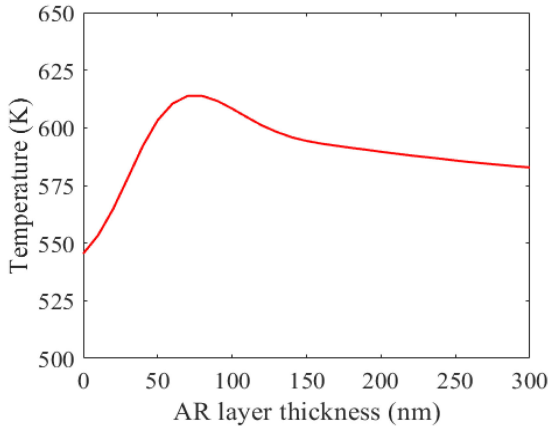

Fig. 5. Equilibrium temperature versus the AR layer thickness for the dielectric layer on metal structure. Highest equilibrium temperature of 614 K is predicted at the aluminum oxide dielectric layer thickness of 75 nm. The bottom metal is a 200 nm thick tungsten film in calculations.

(AR) layer thicknesses. In the calculations, the optically thick metal layer is a 200 nm thick tungsten film. Calculated thermal emissivity of thin film structure materials versus wavelength and emission angle for different AR layer thicknesses (50 nm, 70 nm, 90 nm, and 110 nm) is plotted in Fig. 4. It is seen that increasing the AR layer thickness results in increased thermal emissivity in the infrared spectral region.

To optimize the dielectric AR layer thickness for high equilibrium temperature, we calculate equilibrium temperature of zero-bilayer structure with different aluminum oxide dielectric layer thicknesses with the thermal emissivity data obtained by using Kirchhoff's law of thermal radiation. Fig. 5 shows the calculated equilibrium temperature of the zero-bilayer structure versus AR layer thickness. It is seen that the equilibrium temperature increases from 545 K to 614 K as the AR layer thickness is increased from 0 nm to 75 nm. Further increasing AR layer thickness decreases equilibrium temperature. At the AR layer thickness of 300 nm, the equilibrium temperature decreases to

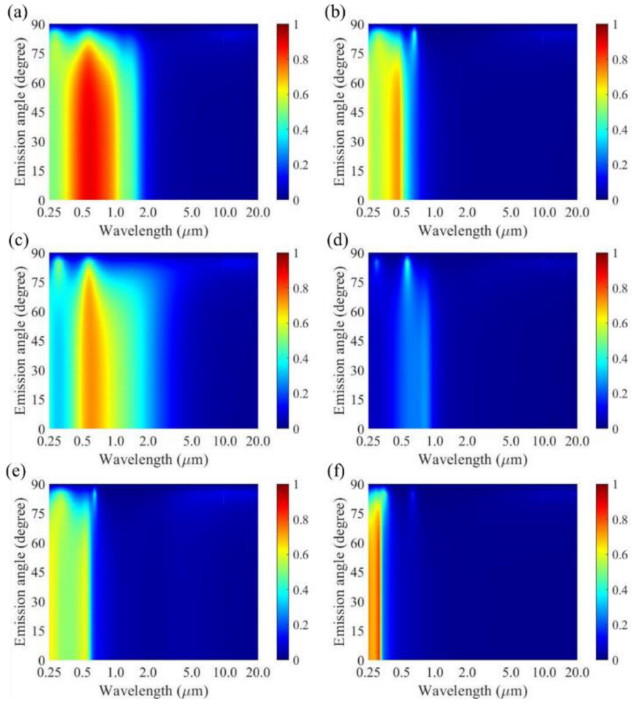

Fig. 6. Calculated thermal emissivity versus wavelength and emission angle for the single AR layer on different metals: (a) Tungsten (W), (b) Gold (Au), (c) Chromium (Cr), (d) Aluminum (Al), (e) Copper (Cu), and (f) Silver (Ag).

583 K. The AR layer thickness of aluminum oxide for achieving high equilibrium temperature is 75 nm as shown in Fig. 5.

Thermal emissivity of zero-bilayer structure with six different metals as the bottom metal layer materials are calculated at different angles of emission and wavelengths. The bottom thick metal layer thickness is 200 nm in all calculations. The six different metals are gold (Au), chromium (Cr), aluminum (Al), copper (Cu), silver (Ag), and tungsten (W). In our calculations, optical constants of six metals were taken from reference [29]. The AR layer thickness is fixed at 70 nm for all structures. Calculated emissivity versus wavelength and emission angle for structures with different metals is plotted in Fig. 6. Among all structures with six different bottom layer metals, the structure with the tungsten metal layer gives the maximal emissivity over the visible-IR spectral range as shown in Fig. 6(a). The dielectric film on silver surface structure gives the minimal emissivity over the visible and infrared solar light spectrum as shown in Fig. 6(f).

After obtaining the emissivity of the dielectric film on metal structure with six different metals, equilibrium temperatures of the single dielectric film on metal structure are calculated under normal solar optical radiation. Calculated equilibrium temperature versus the dielectric layer thickness for six different materials of the thick metal layer are plotted in Fig. 7. It is seen that a 75 nm thickness AR layer on a thick tungsten film can produce a maximal equilibrium temperature of 614 K, while a 45 nm thickness dielectric AR layer on the gold surface can produce a maximal equilibrium temperature of 536 K. The dielectric film on silver structure produce a lowest equilibrium temperature among six different metals. The explanation is that tungsten has the best absorption performance and silver has

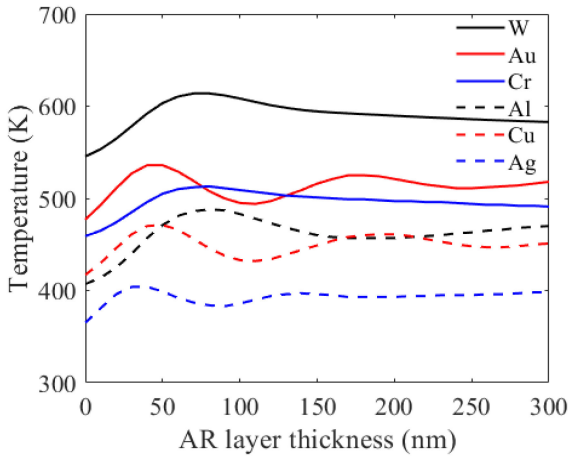

Fig. 7. Calculated equilibrium temperature versus antireflection aluminum oxide dielectric layer thickness for the dielectric layer on metal structure with six different metals: tungsten (W), gold (Au), chromium (Cr), aluminum (Al), copper (Cu), and silver (Ag). The structure with tungsten as the bottom metal produces the highest equilibrium temperature at the layer thickness of 75 nm.

the poorest absorption within the visible solar light spectrum. Meanwhile, all metal structures have similar thermal emissivity in the infrared spectrum range. Therefore, among structures of six different metals in bottom, the structure with tungsten metal produces the highest equilibrium temperature. The structure with silver metal produces the lowest equilibrium temperature under direct solar light radiation. In the calculations, it is assumed that there is no thermal energy loss in the substrate. In reality, there is always some thermal conduction energy loss in the substrate which reduces the equilibrium temperature of the structures. However, the substrate can be insulated to minimize thermal energy loss from the substrate.

VI. Conclusion

In this work, equilibrium temperatures of metal-dielectric multilayer thin film structure metamaterials under direct solar optical radiation were investigated by using Kirchhoff's law. It was found that although increasing the number of metal-dielectric thin-film bilayers can produce wide absorption band and high absorptance, increasing the number of thin film layers does not produce higher equilibrium temperature, because increasing the number of layers also increases the thermal emission in the infrared spectrum region. Counter-intuitively, the structure consisting of a single dielectric layer on metal (DLM) surface can produce highest equilibrium temperature under direct solar light radiation. Additionally, we have shown that tungsten is the best choice of absorbing metal material for producing high equilibrium temperatures.

References

[1] K. D. Olson and J. J. Talghader, "Absorption to reflection transition in selective solar coatings," *Opt. Exp.*, vol. 20, pp. A554–A559, 2012.
[2] J. Chen, L.-Y. Chen, and J. Guo, "Equilibrium temperature of a spectral selective solar light absorber with angular dependent thermal emissivity," *J. Opt. Soc. Amer. B*, vol. 37, pp. 2873–2877, 2020.
[3] J. Chen and J. Guo, "Equilibrium temperature of wideband perfect light absorbers under direct solar illumination," in *Optics/Laser Science*. Optica Publishing Group, 2018.
[4] W. X. Zhou *et al.*, "Nano-Cr-film-based solar selective absorber with high photo-thermal conversion efficiency and good thermal stability," *Opt. Exp.*, vol. 20, pp. 28953–28962. 2012.
[5] X.-F. Li *et al.*, "High solar absorption of a multilayered thin film structure," *Opt. Exp.*, vol. 15, pp. 1907–1912, 2007.
[6] E.-T. Hu *et al.*, "Multilayered metal-dielectric film structure for highly efficient solar selective absorption," *Mater. Res. Exp.*, vol. 1, 2018, Art. no. 066428.
[7] J. Chen, J. Guo, and L.-Y. Chen, "Super-wideband perfect solar light absorbers using titanium and silicon dioxide thin-film cascade optical nanocavities," *Opt. Mater. Exp.*, vol. 6, pp. 3804–3813, 2016.
[8] M.-H. Liu *et al.*, "High efficiency of photon-to-heat conversion with a 6-layered metal/dielectric film structure in the 250-1200 nm wavelength region," *Opt. Exp.*, vol. 22, pp. A1843–A1852, 2014.
[9] S. Zhao and E. Wäckelgård, "Optimization of solar absorbing three-layer coatings," *Sol. Energy Mater. Sol. Cells*, vol. 90, pp. 243–261, 2006.
[10] T. D. Corrigan *et al.*, "Broadband and mid-infrared absorber based on dielectric-thin metal film multilayers," *Appl. Opt.*, vol. 51, pp. 1109–1114, 2012.
[11] C. H. Granier, S. G. Lorenzo, C. You, G. Veronis, and J. P. Dowling, "Optimized aperiodic broadband visible absorbers," *J. Opt.*, vol. 19, 2017, Art. no. 105003.
[12] J. Prentice, "Coherent, partially coherent and incoherent light absorption in thin-film multilayer structures," *J. Phys. D: Appl. Phys.*, vol. 33, 2000, Art. no. 3139.
[13] Z. Li, S. Butun, and K. Aydin, "Large-area, lithography-free super absorbers and color filters at visible frequencies using ultrathin metallic films," *ACS Photon.*, vol. 2, pp. 183–188, 2015.
[14] H. Shen, L. Yang, Y. Jin, and S. He, "Perfect mid-infrared dual-band optical absorption realized by a simple lithography-free polar dielectric/metal double-layer nanostructure," *Opt. Exp.*, vol. 28, pp. 31414–31424, 2020.
[15] A. Lenert *et al.*, "A nanophotonic solar thermophotovoltaic device," *Nature Nanotechnol.*, vol. 9, pp. 126–130, 2014.
[16] W. Li and S. Fan, "Nanophotonic control of thermal radiation for energy applications," *Opt. Exp.*, vol. 26, pp. 15995–16021, 2018.
[17] S. Basu, Z. Zhang, and C. Fu, "Review of near-field thermal radiation and its application to energy conversion," *Int. J. Energy Res.*, vol. 33, pp. 1203–1232, 2009.
[18] X. Liu, L. Wang, and Z. M. Zhang, "Near-field thermal radiation: Recent progress and outlook," *Nanoscale Microscale Thermophysical Eng.*, vol. 19, pp. 98–126, 2015.
[19] T. Inoue, M. De Zoysa, T. Asano, and S. Noda, "Realization of narrowband thermal emission with optical nanostructures," *Optica*, vol. 2, pp. 27–35, 2015.
[20] S.-Y. Lin, J. Fleming, E. Chow, J. Bur, K. Choi, and A. Goldberg, "Enhancement and suppression of thermal emission by a three-dimensional photonic crystal," *Phys. Rev. B*, vol. 62, 2000, Art. no. R2243.
[21] E. Radziemska, "The effect of temperature on the power drop in crystalline silicon solar cells," *Renewable Energy*, vol. 28, no. 1, pp. 1–12, 2003.
[22] P. Singh and N. M. Ravindra, "Temperature dependence of solar cell performance—An analysis," *Sol. Energy Mater. Sol. Cells*, vol. 101, pp. 36–45, 2012.
[23] W. Tress *et al.*, "Performance of perovskite solar cells under simulated temperature-illumination real-world operating conditions," *Nature Energy*, vol. 4, no. 7, pp. 568–574, 2019.
[24] G. Kirchhoff, "I. On the relation between the radiating and absorbing powers of different bodies for light and heat," *London, Edinburgh, Dublin Philos. Mag. J. Sci.*, vol. 20, pp. 1–21, 1860.
[25] W. C. Snyder, Z. Wan, and X. Li, "Thermodynamic constraints on reflectance reciprocity and Kirchhoff's law," *Appl. Opt.*, vol. 37, pp. 3464–3470, 1998.
[26] F. Kelly, "On Kirchhoff's law and its generalized application to absorption and emission by cavities," in *Proc. 2nd Aerosp. Sci. Meeting*, 1965, pp. 126–135.
[27] P.-M. Robitaille, "Kirchhoff's law of thermal emission: 150 years," *Prog. Phys.*, vol. 4, pp. 3–13, 2009.
[28] P. Yeh, *Optical Waves in Layered Media*, Wiley, 2005.
[29] E. D. Palik, *Handbook of Optical Constants of Solids*, Academic, 1998.
[30] M. Planck, *The Theory of Heat Radiation*. Blakiston, 1914.
[31] *Standard Tables for Reference Solar Spectral Irradiances: Direct Normal and Hemispherical on 37° Tilted Surface*, West Conshohocken, PA, USA: ASTM International, 2020, ASTM G173-03. [Online]. Available: www.astm.org